Principles of CT: Multislice CT*

Lee W. Goldman

Department of Radiation Therapy and Medical Physics, Hartford Hospital, Hartford, Connecticut

This article describes the principles and evolution of multislice CT (MSCT), including conceptual differences associated with slice definition, cone beam effects, helical pitch, and helical scan technique. MSCT radiation dosimetry is described, and dose issues associated with MSCT—and with CT in general—as well as techniques for reducing patient radiation dose are discussed. Factors associated with the large volume of data associated with MSCT examinations are presented.

Key Words: CT; multislice CT; radiation dosimetry

J Nucl Med Technol 2008; 36:57–68
DOI: 10.2967/jnmt.107.044826

This article, the third in a series of continuing education articles on the principles of CT, focuses on multislice CT (MSCT).

PRINCIPLES OF MSCT

Limitations of Single-Slice Slip Ring and Helical Scanners

Soon after their introduction in the late 1980s, slip ring scanners and helical (spiral) CT were rapidly adopted and soon became the de facto standard of care for body CT. However, a significant problem became evident: helical CT was very hard on x-ray tubes. For example, an abdomen–pelvis helical CT covering 60 cm (600 mm) of anatomy with a 5-mm slice thickness, a pitch of 1.0 (thus requiring 120 rotations), and typical technique factors (120 kilovolts [peak] [kVp], 250 mA, 1-s rotation time) deposits a total of 3.6×10^6 J of heat in the x-ray tube anode. Before slip ring CT, individual slices obtained with an equivalent technique (120 kVp, 250 mA, 1-s scan) would deposit only 30,000 J, much of which could be dissipated during the relatively lengthy (several seconds) interscan delay.

A limitation imposed by tube heating was that the thin slices (<3 mm) desired for acceptable-quality reformatting into off-axis images (coronal, sagittal, or oblique) or 3-dimensional reconstructions were impractical unless the scanned region was very limited or the scan technique was severely constrained. It was not uncommon for scanners to limit a helical technique with thin slices to 100 mAs (tube current in milliamperes × scan time in seconds) or less per rotation, yielding low-quality, noisy images.

A straightforward solution to this heat issue, of course, is to develop x-ray tubes with a higher heat capacity; such tubes have been asnd continue to be developed. Another approach is to more effectively use the available x-ray beam: if the x-ray beam is widened in the *z*-direction (slice thickness) and if multiple rows of detectors are used, then data can be collected for more than one slice at a time. This approach would reduce the total number of rotations—and therefore the total usage of the x-ray tube—needed to cover the desired anatomy. This is the basic idea of MSCT.

Although both third- and fourth-generation scanners were in common use as single-slice scanners, all multislice scanners are based on a third-generation platform. Therefore, in the following discussion, third-generation scanner geometry (tube and detector bank linked and rotating together) is assumed.

MSCT Detectors

The primary difference between single-slice CT (SSCT) and MSCT hardware is in the design of the detector arrays, as illustrated in Figure 1. SSCT detector arrays are one dimensional (Fig. 1); that is, they consist of a large number (typically 750 or more) of detector elements in a single row across the irradiated slice to intercept the x-ray fanbeam. In the slice thickness direction (*z*-direction), the detectors are monolithic, that is, single elements long enough (typically about 20 mm) to intercept the entire x-ray beam width, including part of the penumbra (here, the term "x-ray beam width" always refers to the size of the x-ray beam along the *z*-axis—that is, in the slice thickness direction). In MSCT, each of the individual, monolithic SSCT detector elements in the *z*-direction is divided into several smaller detector elements, forming a 2-dimensional array (Fig. 1). Rather than a single row of detectors encompassing the fanbeam, there are now multiple, parallel rows of detectors.

Before further discussion, a comment on nomenclature is called for: the use of the term "MSCT" is not universal. Others use the terms "multirow CT" and "multidetector

Received Jul. 24, 2007; revision accepted Dec. 4, 2007.
For correspondence or reprints contact: Lee W. Goldman, Department of Radiation Therapy and Medical Physics, Hartford Hospital, 80 Seymour St., Hartford, CT 06102.
E-mail: lgoldma@harthosp.org
*NOTE: FOR CE CREDIT, YOU CAN ACCESS THIS ACTIVITY THROUGH THE SNM WEB SITE (http://www.snm.org/ce_online) THROUGH June 2010.

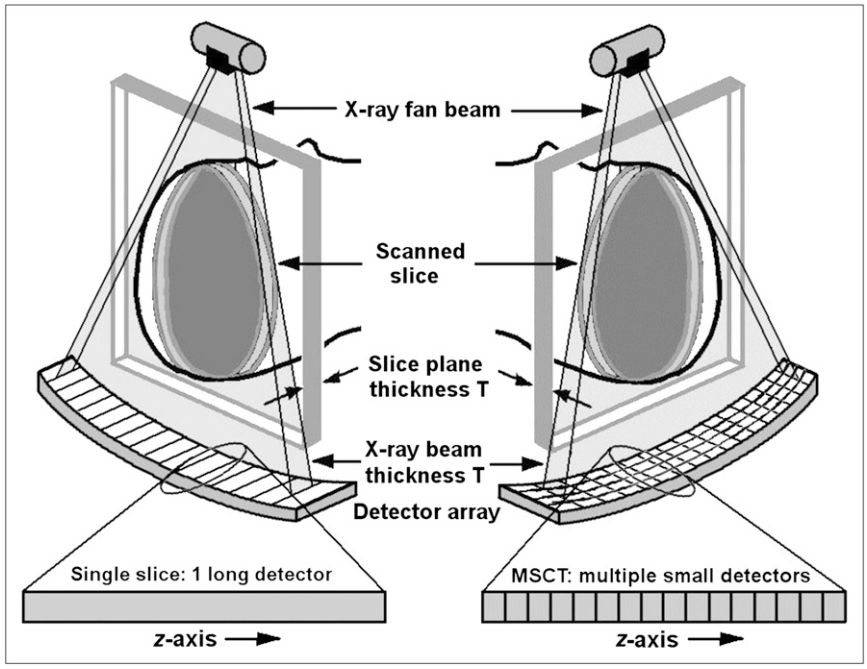

FIGURE 1. (Left) SSCT arrays containing single, long elements along *z*-axis. (Right) MSCT arrays with several rows of small detector elements.

row CT (MDCT)" because they are more descriptive of this technology than the term "multislice CT." Throughout this article, however, the term "MSCT" is used.

The first scanner with more than one row of detectors and a widened *z*-axis x-ray beam was introduced by Elscint in 1992 (CT-Twin). This scanner had 2 rows of detectors, allowing data for 2 slices to be acquired simultaneously, and was developed primarily to help address the x-ray tube heating problem. As a curious historical note, according to the description given earlier in this article, the first MSCT scanner would actually be the first-generation EMI Mark 1. With 2 adjacent detectors and a widened x-ray beam, this scanner collected data for 2 slices at the same time and thereby reduced the lengthy examination time associated with the 5- to 6-min scan time (*1*). The first scanners of the "modern MSCT era" were introduced in late 1998 and are described in the following discussion (*1*).

MSCT Data Acquisition

A detector design used in one of the first modern MSCT scanners (Fig. 1) consisted of 16 rows of detector elements, each 1.25 mm long in the *z*-direction, for a total *z*-axis length of 20 mm. Each of the 16 detector rows could, in principle, simultaneously collect data for 16 slices, each 1.25 mm thick; however, this approach would require handling an enormous amount of data very quickly, because a typical scanner may acquire 1,000 views per rotation. If there are 800 detectors per row and 16 rows, then almost 13 million measurements must be made during a single rotation with a duration of as short as 0.5 s.

Because of the initial limitations in acquiring and handling such large amounts of data, the first versions of modern MSCT scanners limited simultaneous data acquisition to 4 slices. Four detector "rows" corresponding to the 4 simultaneously collected slices fed data into 4 parallel data "channels," so that these 4-slice scanners were said to possess 4 data channels. These 4-slice scanners, however, were quite flexible with regard to how detector rows could be configured; groups of detector elements in the *z*-direction could be electronically linked to function as a single, longer detector, thus providing much flexibility in the slice thickness of the 4 acquired slices. Examples of detector configurations used with the 4 channels are illustrated in Figure 2 for 2 versions of 4-slice MSCT detectors: one based on the detector design described earlier (16 rows of 1.25-mm elements) and the other based on an "adaptive array" consisting of detector elements of different sizes (other detector designs were used by other manufacturers) (*2,3*).

Possible detector configurations for the detector design encompassing 16 rows of 1.25-mm elements for the acquisition of 4 slices are illustrated in Figures 2A and 2B. In Figure 2A, 4 elements in a group are linked to act as a single 5-mm detector (4×1.25). The result is four 5-mm detectors covering a total *z*-axis length of 20 mm. When a 20-mm-wide x-ray beam is used, 4 slices with a thickness of 5 mm are acquired. The acquired 5-mm slices can also be combined into 10-mm slices, if desired. In Figure 2B, 4 pairs of detector elements are linked to function as four 2.5-mm detectors (2×1.25). When a 10-mm-wide x-ray beam is used, four 2.5-mm slices can be acquired simultaneously. Again, the resulting 2.5-mm slices can be combined to form 5-mm slices (5-mm axial slices are generally preferred for interpretation purposes). A third possibility is to use a 5-mm-wide x-ray beam to irradiate only the 4 innermost individual detector elements for the acquisition of four 1.25-mm slices. Yet another possibility is to link

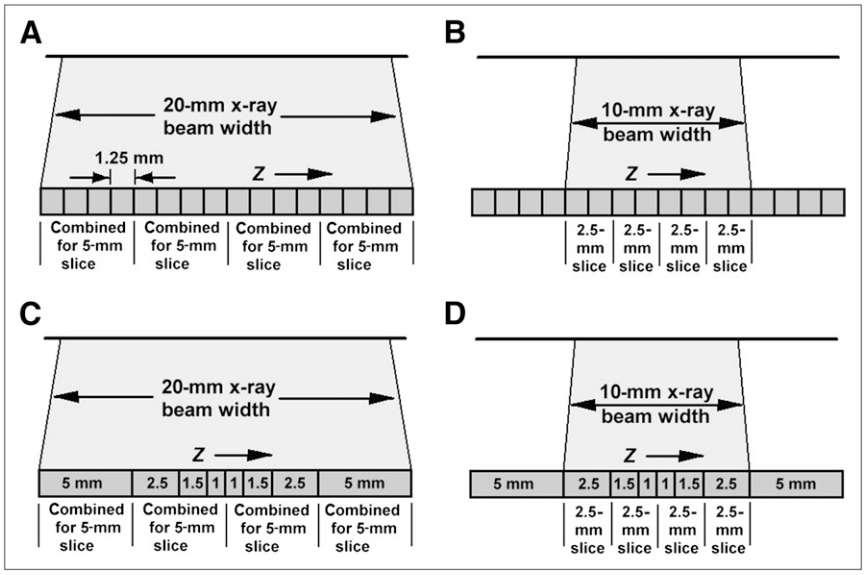

FIGURE 2. Flexible use of detectors in 4-slice MSCT scanners. (A) Groups of four 1.25-mm-wide elements are linked to act as 5-mm-wide detectors. (B) Inner 8 elements are linked in pairs to act as 2.5-mm detectors. (C) Inner, adaptive-array elements are linked to act as 5-mm detectors (1 + 1.5 + 2.5) and, together with outer, 5-mm elements, yield four 5-mm slices. (D) The 4 innermost elements are linked in pairs to form 2.5-mm detectors (1 + 1.5), which along with the two 2.5-mm detectors, collect data for four 2.5-mm slices.

elements in triplets and use a 15-mm-wide x-ray beam to acquire four 3.75-mm slices.

Similarly, the individual elements of the adaptive array can be appropriately linked to acquire four 5-mm slices (Fig. 2C) or four 2.5-mm slices (Fig. 2D). Another possibility is to use a 4-mm-wide x-ray beam (which would irradiate only part of the 1.5-mm elements) to yield four 1-mm slices. Thinner slices can be combined to form thicker slices for interpretation purposes, if necessary.

As data acquisition technology advanced, more data channels were provided to allow the simultaneous acquisition of more than 4 slices. An 8-channel version of the system encompassing the detector array in Figures 2A and 2B (introduced approximately 3 y later) could acquire eight 2.5-mm slices or eight 1.25-mm slices (which could be combined to form thicker slices for interpretation).

Submillimeter Slices and Isotropic Resolution

The 4-slice and 8-slice MSCT scanners just described were also capable of acquiring ultrathin ("submillimeter") slices (but only 2 at a time) by collimating the x-ray beam in the *z*-axis to partially irradiate the 2 innermost detector elements in the detector array. For example, for the detector array in Figure 2A, if the x-ray beam is collimated to a 1.25-mm width and aligned so as to straddle and partially irradiate the 2 innermost detector elements, then 2 slices, each 0.625 mm thick, can be obtained. When images resulting from such an acquisition are reformatted into sagittal, coronal, or other off-axis images, the reformatted images exhibit spatial resolution in the *z*-direction that is essentially equal to that within the plane of the axial slices. Resolution that is (essentially) equal in all 3 directions is said to be isotropic.

Because only 2 submillimeter slices could be acquired simultaneously with these earlier MSCT scanners, this capability was not widely used because of limited *z*-axis coverage and tube heating limitations. Submillimeter scanning had to await the introduction of 16-slice scanners.

16-Channel (16-Slice) Scanners—and More

The installation of MSCT scanners providing 16 data channels for 16 simultaneously acquired slices began in 2002. In addition to simultaneously acquiring up to 16 slices, the detector arrays associated with 16-slice scanners were redesigned to allow thinner slices to be obtained as well. Detector arrays for various 16-slice scanner models are illustrated in Figure 3. Note that in all of the models, the innermost 16 detector elements along the *z*-axis are half the size of the outermost elements, allowing the simultaneous acquisition of 16 thin slices (from 0.5 mm thick to 0.75 mm thick, depending on the model). When the inner detectors were used to acquire submillimeter slices, the total acquired *z*-axis length and therefore the total width of the x-ray beam ranged from 8 mm for the Toshiba version to 12 mm for the Philips and Siemens versions. Alternatively, the inner 16

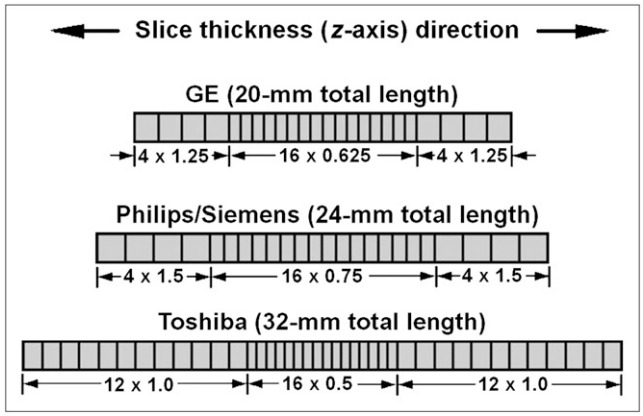

FIGURE 3. Diagrams of various 16-slice detector designs (in *z*-direction). Innermost elements can be used to collect 16 thin slices or linked in pairs to collect thicker slices.

elements could be linked in pairs for the acquisition of 16 thicker slices (*4*).

During 2003 and 2004, MSCT manufacturers introduced models with both fewer than and more than 16 channels. Six-slice and 8-slice models were introduced by manufacturers as cost-effective alternatives. At the same time, 32-slice and 40-slice scanners were being introduced.

By 2005, 64-slice scanners were announced, and installations by most manufacturers began. Detector array designs used by several manufacturers are illustrated in Figure 4. The approach used by most manufacturers for 64-slice detector array designs was to lengthen the arrays in the *z*-direction and provide all submillimeter detector elements: 64 × 0.625 mm (total *z*-axis length of 40 mm) for the Philips and GE Healthcare models and 64 × 0.5 mm (total *z*-axis length of 32 mm) for the Toshiba model. The design approach of Siemens was quite different. The detector array of the Siemens 32-slice scanner (containing 32 elements each 0.6 mm long, for a total *z*-axis length of 19.2 mm) was combined with a "dynamic-focus" x-ray tube for the simultaneous acquisition of 64 slices. This x-ray tube could electronically—and very quickly—shift the focal spot location on the x-ray tube target so as to emit radiation from a slightly different position along the *z*-axis. Each of the 32 detector elements then collected 2 measurements (samples), separated along the *z*-axis by approximately 0.3 mm. The net result was a total of 64 measurements (32 detectors × 2 measurements per detector) along a 19.2-mm total *z*-axis field of view (this process is referred to in Siemens literature as "Z-Sharp" technology) (*5*).

In the preceding examples, in addition to the simultaneous acquisition of more slices, MSCT x-ray beam widths can be considerably wider than those for SSCT. Sixteen-slice MSCT beam widths are up to 32 mm; 64-slice beams can be up to 40 mm wide; and even wider beams are used in systems currently under development or in clinical evaluation. A possible consequence is that more scatter may reach the detectors, compromising low-contrast detection. Generally, however, the antiscatter septa traditionally used with third-generation CT scanners can be made sufficiently deep to remain effective with MSCT. An example of a section of a 16-slice detector with the associated scatter removal septa is shown in Figure 5.

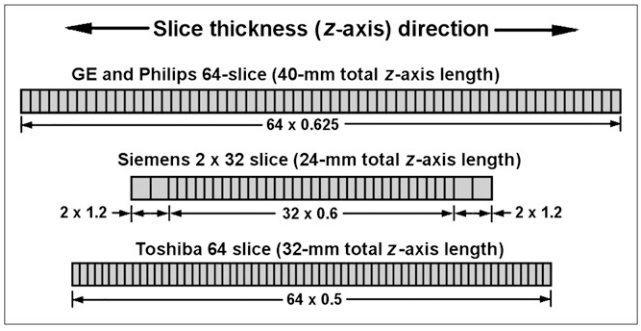

FIGURE 4. Diagrams of various 64-slice detector designs (in *z*-direction). Most designs lengthen arrays and provide all submillimeter elements. Siemens scanner uses 32 elements and dynamic-focus x-ray tube to yield 2 measurements per detector.

MSCT CONCEPTS: DIFFERENCES BETWEEN MSCT AND SSCT

Before the further development of MSCT technology is described, certain concepts that are associated with MSCT and that may differ fundamentally from those associated with SSCT are addressed. One of these concepts is the relationship between slice thickness and x-ray beam width. Another involves the notion of cone beam effects.

MSCT Slice Thickness and X-Ray Beam Collimation

In SSCT, slice thickness is determined by prepatient and possibly postpatient x-ray beam collimators. Generally, the x-ray beam collimation was designed such that the *z*-axis width of the x-ray beam at the isocenter (i.e., at the center of rotation) is the same as the desired slice thickness. (The x-ray beam width, usually defined as the full width at half maximum [FWHM] of the *z*-axis x-ray beam intensity profile, is discussed in detail in the second article in this series (*6*).)

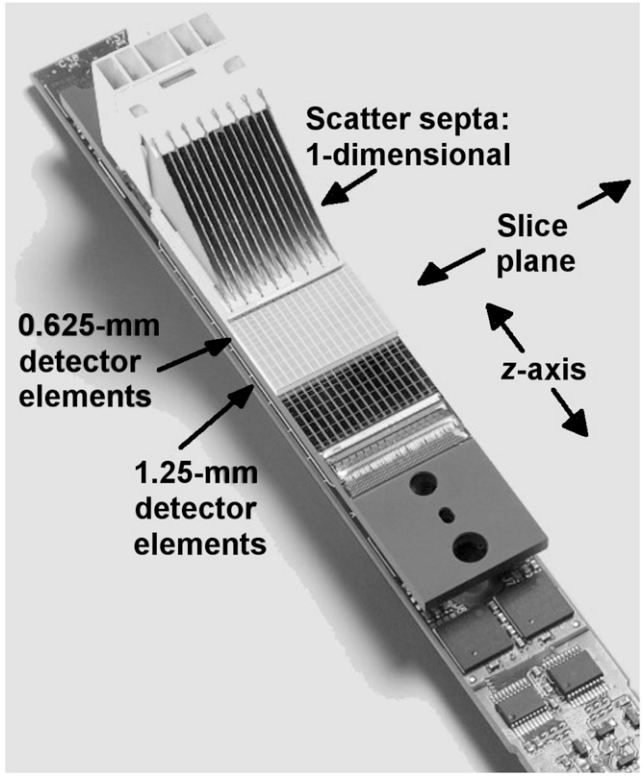

FIGURE 5. Section of 16-slice detector with scatter removal septa. Septa are sufficiently deep to eliminate nearly all scatter. Note smaller elements (0.625 mm, in this example) in center of array and larger (1.25-mm) outer elements. Also note dead spaces (lighter lines) between elements.

In MSCT, however, slice thickness is determined by detector configuration and not x-ray beam collimation. For example, the 4 slices in Figure 2A are each 5 mm thick because they are acquired by 5-mm detectors (formed by linking four 1.25-mm detector elements). The 4 slices in Figure 2B are 2.5 mm thick because they are acquired by 2.5-mm detectors (formed by linking two 1.25-mm elements). Because it is the length of the individual detector (or linked detector elements) acquiring data for each of the simultaneously acquired slices that limits the width of the x-ray beam contributing to that slice, this length is often referred to as detector collimation. In Figures 2A and 2C, the detector collimation is 5 mm. In Figures 2B and 2D, the detector collimation is 2.5 mm. The actual x-ray beam collimation is not directly involved in determining slice thickness, other than that the "total" *z*-axis beam collimation should be equal to the total thickness of the 4 slices, for example, 20 mm in Figure 2A or 10 mm in Figure 2B (that this is not necessarily true is discussed in the MSCT dosimetry section later in this article) (*7*).

Cone Beam Effects in MSCT

Cone beam effects in CT are associated with the divergent nature of the x-ray beam emitted from the x-ray tube. This divergence means that the *z*-axis of the x-ray beam is somewhat wider when it exits the patient than when it entered the patient.

In SSCT, the main consequence of x-ray beam divergence is the potential for partial-volume streaking, discussed in the second article in this series (*6*) and reviewed here. During a 360° rotation, the same path (or nearly the same path) of x-rays through the patient is measured twice, but with x-rays traveling in opposite directions, for example, once with the tube above the patient and detectors below and later on during the rotation with the tube below the patient and the detectors above (these are referred to as parallel opposed rays or conjugate rays). Because of beam divergence, however, the cone-shaped x-ray beam samples slightly different tissue volumes in each direction (Fig. 6A), potentially leading to data inconsistencies and streak artifacts. The thicker the slice (the wider the x-ray beam), the more pronounced the divergence and the more likely it is that parallel opposed ray measurements will be inconsistent.

Cone beam effects are more severe in MSCT. Consider the MSCT configuration in Figure 6B, collecting data for eight 2.5-mm slices (total beam width of 20 mm). Note that the measurements obtained with the outermost detector (shading in Fig. 6B) from opposite sides of the patient not only sample different tissues but also do not even lie within the same slice (*3*).

With 4-slice scanners, the total x-ray beam width was sufficiently narrow (e.g., 5 mm wide for four 1.25-mm slices) or else the slices were sufficiently thick (four 5-mm slices) that cone beam effects were tolerable and conventional filtered backprojection reconstruction was still usable. However, MSCT scanners of later generations, which collected more and thinner slices, required the development of alternate cone beam reconstruction algorithms (which are beyond the scope of this article). Because of cone beam effects, some MSCT scanners with 16 channels or more only allow the simultaneous acquisition of the maximum number of slices (e.g., 16 slices by a 16-channel scanner) during helical scans and prevent such acquisitions during axial (nonhelical) scans.

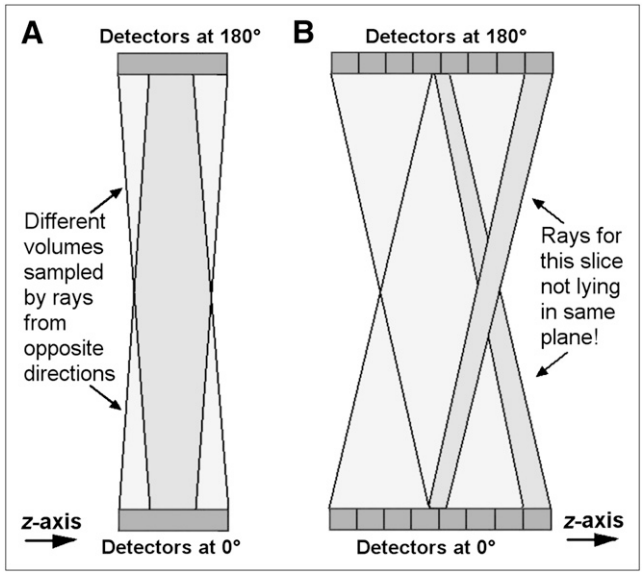

FIGURE 6. Cone beam effects in SSCT and MSCT. (A) In SSCT, divergent, cone-shaped x-ray beam irradiates different tissues—yielding different attenuation measurements—for parallel opposed rays, sometimes causing streaking for thicker slices. (B) Wider beams of MSCT accentuate cone beam shape and lead to rays that do not even lie within same plane. Cone beam reconstruction algorithms are generally required. opp. = opposite.

HELICAL MSCT

Helical scanning with MSCT scanners is conceptually identical to that with SSCT scanners; rotation and table movement occur simultaneously with continuous data acquisition. However, certain terminology, along with peculiarities associated with helical pitch selection and helical slice reconstruction, tends to cause confusion. A discussion of the concept of helical pitch follows.

Definition of Pitch Revisited

As originally defined for SSCT, helical pitch was calculated as table movement per rotation divided by slice thickness. For example, with a slice thickness of 5 mm and a table movement of 7.5 mm per rotation, pitch would be 1.5. Because slice thickness and x-ray beam width are equivalent in SSCT, the value for pitch conveyed important information about the x-ray beam; a pitch of 1.0 meant that the x-ray beams from adjacent rotations were essentially contiguous. Pitches of greater than 1 implied gaps between the x-ray beams from adjacent rotations. Pitches of less

than 1 implied x-ray beam overlap (and thus double irradiation of some tissue) and so were not clinically used.

Applying this definition to MSCT creates confusion and tends to obscure important information. For example, a 4-slice MSCT helical scan with 15 mm of table movement per rotation and a 20-mm-wide x-ray beam (to acquire four 5-mm slices) would yield the following pitch calculation based on the earlier definition: pitch = table movement per rotation/slice thickness = 15 mm/5 mm = 3.0. This calculation does not immediately convey the fact that although the pitch is much greater than 1, there is clearly x-ray beam overlap, because the total width of the x-ray beam is 20 mm and the table is moving only 15 mm per rotation. To address this situation, a new definition of pitch was adopted. In this definition, the denominator is replaced with the total thickness of all of the simultaneously acquired slices; that is, if n slices each of slice thickness T are acquired, then the total width is $n \times T$, and the new pitch definition is as follows: pitch = table movement per rotation/($n \times T$) (beam pitch). Because the original definition is still occasionally referenced, the new pitch definition in the latter equation is called "beam pitch." The original definition is now referred to as "detector pitch," on the basis of the idea that slice thickness (in the denominator of the original definition) in MSCT is determined by detector configuration. With the new definition, beam pitch for the example just given would be calculated as follows: pitch = table movement per rotation/($n \times T$) = 15 mm/(4 × 5 mm) = 0.75. Because beam pitch conveys similar information for MSCT as the original definition did for SSCT, it is the preferred definition in most situations (*2*).

Pitch and z Sampling in Helical MSCT

Clinical pitch selection in SSCT was generally straightforward. Typically, only 2 pitches were commonly used: pitch = 1 for best quality and pitch = 1.5 when more z-axis coverage was needed in a shorter time (because of either total scan time or x-ray tube heating constraints). Pitches of less than 1 were not used. In contrast, commonly used beam pitches in MSCT may seem odd (e.g., 0.9375, 1.125, or 1.375) and are very often less than 1. Before helical pitch in MSCT is discussed, the basic trade-off involving pitch selection is reviewed (see the first article in this series (*8*) for a more complete discussion).

Because of continuous table movement, no specific slice position along the z-axis actually contains sufficient data (i.e., transmission measurements along ray paths through the slice at sufficient locations and angles) to reconstruct an image. Rather, required measurements are estimated by interpolation between the nearest measurements above and below the slice plane that are at the same relative position and angle. The distance along the z-axis between these measurements that is available for interpolation is referred to here as the z-spacing. Interpolated data may be inaccurate if anatomy changes significantly within the z-spacing, leading to streak or shading artifacts. Helical interpolation artifacts often appear as (and are referred to as) "windmill" artifacts, because when the helical images are paged through quickly, the streak or shading artifacts seem to rotate like the vanes of a windmill. The likelihood and severity of helical artifacts increase with increasing z-spacing, because anatomy is more likely to change abruptly over distance. Increasing pitch (to reduce either scan time or x-ray tube heating) increases distance between interpolated measurements, so that the likelihood of helical artifacts increases.

In helical SSCT, slice data are interpolated between equivalent rays separated by a full rotation (360° apart) or between parallel opposed rays (180° apart). These 2 interpolation schemes are referred to as 360° linear interpolation (360° LI) and 180° linear interpolation (180° LI), respectively. Because parallel opposed rays in SSCT interleave those separated by 360°, z-spacing for 180° LI averages half that for 360° LI (Appendix A provides clarification of this statement). Because of its smaller z-spacing and therefore reduced helical artifacts, 180° LI is generally preferred over 360° LI. z-Spacing in helical SSCT is minimized by use of 180° LI and a pitch of 1 (assuming that pitches of less than 1 are avoided), in which case the average z-spacing equals d/2, where d is the slice thickness (Fig. 7A) (*9*).

In MSCT, 180° LI and a pitch of 1 does not improve z-spacing, as demonstrated by the 4-slice example in Figure 7B. With detector collimation represented as "d," the detectors move relative to the patient by 4d (4 slice thicknesses) in one full 360° rotation. After a half rotation (180°), the detectors move 2d. Unlike the situation in SSCT, 180° opposed rays now duplicate, rather than interleave, those separated by a full rotation, resulting in a z-spacing equal to d. Suppose, instead, that a value of 3d (3 slice thicknesses) is used (Fig. 7C); then, 180° opposed rays interleave those 360° apart and provide a z-spacing of d/2, equivalent to that achieved in SSCT with a pitch of 1 and the same slice thickness. A "rule" for this particular scheme is to overlap one detector width (one slice thickness). For the 4-slice example, this corresponds to a pitch of 3/4 = 0.75; for a 16-slice scanner, the pitch is 15/16 = 0.9375; and for a 64-slice scanner, the pitch is 63/64 = 0.9844. Note that such pitches move closer to 1 (smaller fraction of beam overlap) as the number of simultaneously acquired slices increases (more information regarding this point is provided later in this article) (*10*).

Selection of Helical MSCT Pitch and Data Interpolation

Although illustrating why MSCT helical pitches may seem odd or may be less than 1, the "one-detector overlap" method is not necessarily optimal or preferred. Some MSCT scanner manufacturers recommend alternative pitch strategies, whereas still others maintain that with appropriate interpolation procedures, all (reasonable) pitches are equally good (*9,11,12*). The helical scans shown in Figure 8 help clarify these differences and highlight an important distinction between SSCT and MSCT data interpolation. If

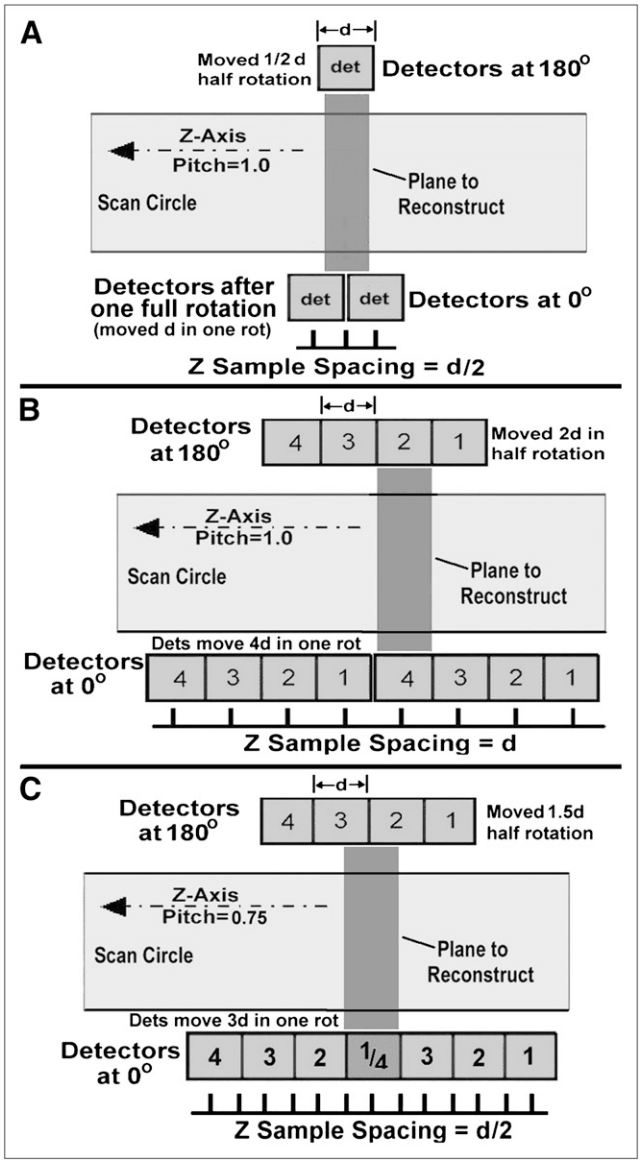

FIGURE 7. *z*-Spacing in helical CT. (A) Minimum *z*-spacing equal to d/2 (d = slice thickness) is achieved in SSCT with pitch of 1 and interpolation between interleaved parallel opposed rays. (B) With pitch of 1 in MSCT, parallel opposed rays overlap rather than interleave, giving *z*-spacing equal to d. (C) *z*-Spacing equivalent to that in SSCT is achieved with pitch that overlaps one slice thickness but results in double irradiation of some tissue. Reduced *z*-spacing can also be achieved with other pitches. det = detector; rot = rotation.

a 4-slice scanner uses a detector configuration of 4 × 5 mm to acquire four 5-mm-thick slices (Fig. 8A), then slice interpolation proceeds as described earlier (usually with 180° LI), preferably with a pitch providing a smaller *z*-spacing (such as the one-detector overlap mentioned earlier) to reduce interpolation artifacts. In Figure 8B, with a detector collimation of 4 × 1.25 mm, 13 detector samples lie completely or partially within the 5-mm slice plane to reconstruct (depending on the slice position relative to the overlapping detectors, 11–13 samples may lie within the slice plane). It is clear that this example no longer involves a simple interpolation between the 2 nearest points but rather requires an appropriate combination of all measurements lying within the slice. With appropriate weighting, these measurements may be combined to form a 5-mm-thick slice measurement with a well-shaped beam profile. This process is referred to as "*z* filtering." With a pitch of 1 rather than 0.75, *z*-spacing increases from 0.625 mm (i.e., d/2) to 1.25 mm (i.e., d) and leads to only minor degradation of the slice profile shape and increased helical artifacts. For 16-slice scanners (and more), the detector collimation during helical scans is 1.5 mm or less (depending on the model and beam width), with correspondingly small differences in the slice profile shape versus pitch.

Helical MSCT Pitch and mAs

Low contrast sensitivity (the ability to resolve low-contrast structures) depends on CT image noise. CT image noise originates primarily from quantum mottling, which depends on the number of x-ray photons contributing to the

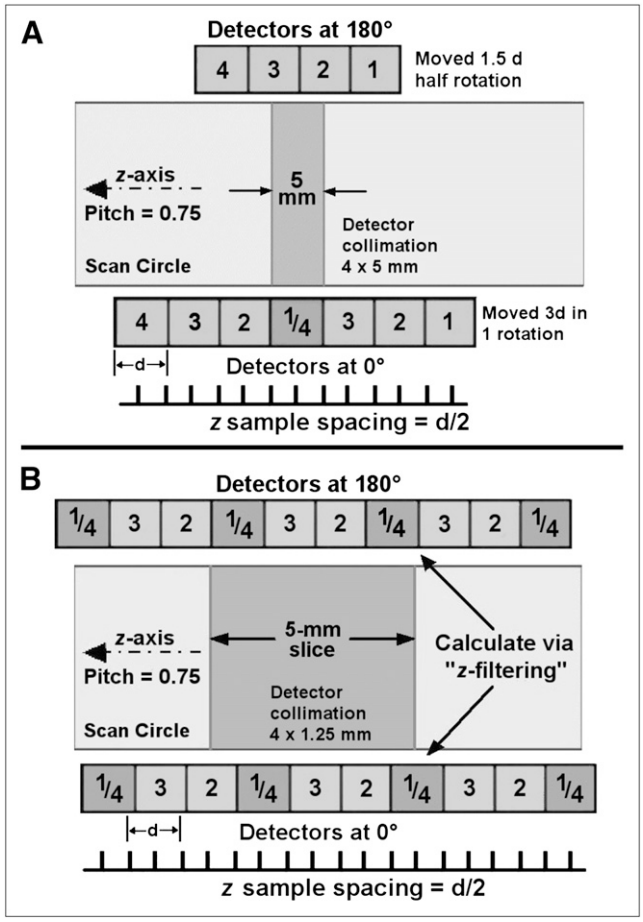

FIGURE 8. *z* Filtering. (A) For MSCT scans configured to acquire thicker slices (e.g., 5 mm), slices are interpolated as for SSCT. (B) For MSCT scans with small detector collimation, numerous measurements are obtained within slice plane (up to 13, in this example) to form thicker slices. Combining many measurements to form thicker slices is referred to as *z* filtering.

image (the appearance of image noise also depends on the sharpness of the reconstruction filter used). To understand how various factors affect CT image noise, it is easiest to consider how many x-ray photons contribute to each detector measurement. Relevant factors include kVp (with higher kVp, more x-rays penetrate the patient to reach the detectors), slice thickness (the detectors collect more photons over thicker slices), x-ray tube mA (a higher x-ray intensity increases the number of detected x-rays proportionally), and rotation time (faster rotation corresponds to shorter detector sampling times). The last 2 factors are often taken together as mAs (see the second article in this series (*6*) for a more complete discussion).

Helical SSCT slices are reconstructed from data interpolated between the 2 nearest parallel ray measurements (usually with 180° LI). Therefore, the number of x-ray photons contributing to each interpolated sample (and therefore to reducing image noise) is a linear combination of 2 detector measurements, regardless of pitch. That is, helical SSCT image noise is unaffected by pitch (*9*). (Note, however, that the interpolation algorithm does affect image noise; fewer rays contribute to images when 180° LI is used than when 360° LI is used, so that 180° LI images are somewhat noisier). Pitch does affect image noise in helical MSCT if slice measurements are formed from many detector samples. For example, the 5-mm slice in Figure 8B is formed from a combination of 11–13 detector measurements. If the average x-ray flux reaching each detector element is n, then the number of x-ray photons contributing to the calculated (z-filtered) sample is between $11n$ and $13n$. In comparison, a pitch of 1.5 and a detector collimation of 4×1.25 mm results in only 5–7 detector measurements lying within the 5-mm slice plane and thus contributing to each slice sample. For the same average detector flux n as that used in the earlier example, the number of contributing x-ray photons is $5n$–$7n$. That is, fewer x-ray photons contribute to each calculated slice sample for larger pitches, leading to noisier images.

In general, the number of photons contributing to images decreases linearly with helical MSCT pitch if the same x-ray technique settings (kVp and mAs) are used. As discussed later in this article, with the same x-ray technique factors, patient radiation dose (CT volume dose index [$CTDI_{vol}$]) also decreases linearly with pitch (in effect, the same amount of energy is spread over more tissue in the z-direction). Therefore, a practice adopted by some manufacturers is to specify "effective" mAs(mAs_{eff}), calculated as

$$mAs_{eff} = mAs/pitch,$$

rather than actual mAs, during examination prescription. mAs_{eff} is chosen to maintain the same level of image noise regardless of selected pitch. For example, with 1-s rotation times, a mAs_{eff} of 240 uses 240 mA with a pitch of 1 ($mAs_{eff} = 240/1 = 240$) but uses 300 mA with a pitch of 1.25 ($mAs_{eff} = 300/1.25$) and 200 mA with a pitch of 0.83 ($mAs_{eff} = 200/0.83$).

MSCT RADIATION DOSIMETRY

Although axial and helical MSCT involves a more complex data collection process, measuring and specifying patient radiation doses in MSCT are no different from in SSCT. For both axial and helical dosimetry purposes, detector collimation is ignored and an MSCT scanner is treated as a single-slice scanner with a slice thickness equal to the full collimated x-ray beam width. For example, an MSCT scan with a detector collimation of 4×2.5 mm (total beam width of 10 mm) would be treated for dosimetry purposes as an SSCT scan with a slice thickness of 10 mm (see the second article in this series (*6*) for a complete discussion of CT dosimetry). For axial scans, therefore, the weighted CTDI [$CTDI_w$] for a detector collimation of 4×2.5 mm (the slices from which may be combined to form 10-mm slices) is equivalent in principle to that of a 10-mm SSCT slice. Similarly, the $CTDI_{vol}$ for helical scans is obtained from axial $CTDI_w$ measurements at the same beam collimation by dividing the axial $CTDI_w$ by the pitch.

There are, however, certain factors that reduce the dose efficiency of MSCT relative to SSCT. In addition, certain MSCT practices that were uncommon or nonexistent in SSCT may lead to increased patient radiation doses. These factors and issues are described in the following discussion.

MSCT Dose Efficiency

Dose efficiency refers to the fraction of x-rays that reach the detectors and that are actually captured and contribute to image formation. Dose efficiency has 2 components: geometric efficiency and absorption efficiency. Absorption efficiency refers to the fraction of x-rays that enter active detector areas and that are actually absorbed (captured). Absorption efficiencies are similar for all SSCT and MSCT scanners that have solid-state detectors. Geometric efficiency refers to the fraction of x-rays that exit the patient and that enter active detector areas.

Two aspects of MSCT reduce its geometric dose efficiency relative to that of SSCT. The first is the obvious necessity for dividers between individual detector elements along the z-axis, which create dead space that did not exist within SSCT detectors in the z-direction (there is, of course, dead space from detector dividers within the slice plane for both SSCT and MSCT). These dividers are visible in Figure 5 as the thin, lighter lines between the small detector elements. Depending on detector design and element size, dead space associated with the dividers can represent up to 20% of the detector surface area. That is, up to 20% of x-rays exiting the patient will strike dead space and not contribute to image formation. Because these dividers must satisfy anti–cross talk and physical separation requirements, divider width generally remains unchanged as detector elements are made smaller (compare the dividers

between the 0.625-mm elements and the 1.25-mm elements in Fig. 5). Therefore, the dividers represent a larger fraction of detector surface area for smaller elements, leading to lower geometric efficiency. Reducing detector element width from 1.25 mm to 0.635 mm or from 1.5 mm to 0.75 mm approximately doubles the amount of dead space. Geometric efficiency loss is fixed by MSCT detector design and cannot be recovered (*7*).

The second factor that reduces MSCT geometric efficiency is associated with the x-ray beam width. In SSCT, the beam width is taken to be the *z*-axis dose profile width measured at the isocenter (i.e., at the axis of rotation) between profile points corresponding to 50% of the maximum intensity (referred to as the FWHM). A collimator is designed such that the profile FWHM corresponds to the desired slice thickness. Figure 9A illustrates such a dose profile for a 10-mm-wide beam used to irradiate an MSCT detector collimation of 4 × 2.5 mm (to acquire four 2.5-mm slices). Four sections of this profile are shaded to emphasize the x-ray flux contributing to each of the 4 slices. Note that the 2 outer slices receive fewer x-rays—and therefore exhibit more quantum mottling—than do the 2 inner slices. This undesirable situation arises because the 2 outer slices are partially irradiated by the dose profile "edges" (which correspond to the beam penumbra). Providing equivalent radiation to all 4 slices requires that the x-ray beam be widened such that all 4 slices are irradiated by the inner, nonpenumbra region, as illustrated in Figure 9B. In effect, the penumbra regions that contributed to SSCT images cannot be used in MSCT and must be discarded (*7*).

The size of the beam penumbra is related to the collimator design and the focal spot size and changes only moderately at different beam widths. As a result, the fractional loss of dose efficiency associated with the discarded penumbra becomes smaller for larger beam widths, because the penumbra represents a smaller fraction of the total x-ray beam width. A consequence is that CTDI values in MSCT are higher for smaller beam collimation values (Table 1). In comparison, CTDI values in SSCT are nearly independent of slice thickness (and thus beam width, as defined earlier), except in certain cases of thin slices (~1 mm) for which the beam width deviates from the earlier definition. As beams become even wider for higher-slice-count scanners (currently up to 40 mm for 64-slice scanners), the geometric efficiency loss associated with the penumbra becomes less and less of a factor.

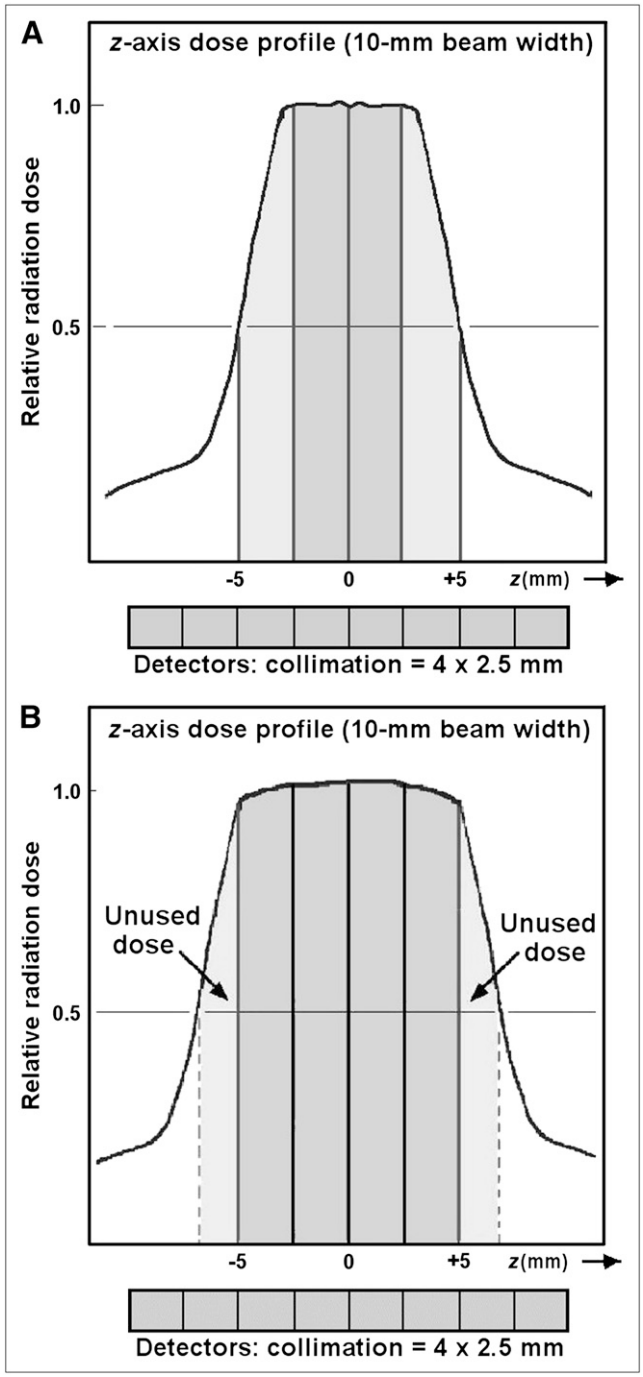

FIGURE 9. Geometric dose efficiency. (A) If MSCT detectors configured to acquire four 2.5-mm slices are irradiated with 10-mm-wide x-ray beam, as specified for SSCT, outer 2 slices will receive lower intensity and yield higher image noise. (B) To compensate, MSCT beams are widened to use only inner, nonpenumbra regions. Penumbra regions that were partially used in SSCT are discarded in MSCT, leading to reduced dose efficiency.

Other Dose-Related Issues in MSCT

As mentioned earlier, helical pitches of less than 1 are sometimes used in MSCT, leading to double irradiation of some tissue. More generally, because $CTDI_{vol}$ increases linearly as pitch is reduced, mAs—and therefore patient dose—should be reduced for smaller pitches to compensate (as mentioned earlier, some systems do this automatically by specifying mAs_{eff} rather than actual mAs).

Other dose-related issues are not specific to MSCT but rather are associated with the rapid growth of CT spawned by MSCT technology and the new applications that it permits. This rapid growth has created increasing concern

TABLE 1
$CTDI_w$ vs. Beam Collimation

Total beam collimation (mm)	Detector configuration	$CTDI_w$ relative to 10-mm beam
5	4 × 1.25 mm	1.22
10	4 × 2.5 mm	1.00
15	4 × 3.75 mm	0.93
20	16 × 1.25 mm	0.89
40	16 × 2.5 mm	0.83

Because discarded penumbra represents smaller fraction of total beam width, CTDI values decrease with increasing beam widths (combined data from GE Healthcare 4-slice and 64-slice MSCT scanners).

about population exposure from CT. Rather than a detailed description of these issues, a brief list of some operational practices to help minimize patient radiation dose is provided here; some of these were described in more detail in the second article in this series (*6*).

Patient Size and Technique Selection. With the same scan technique factors (kVp, mA, rotation time, and slice thickness), patient radiation dose (CTDI) is considerably higher for smaller patients (*13,14*). For example, $CTDI_w$ measured in the standard 16-cm dosimetry phantom (representing a small pediatric patient) is nearly double that measured in the standard 32-cm dosimetry phantom (representing a medium to large patient) with the same technique factors. It is important to adjust mAs appropriately for patients of different sizes, especially pediatric patients. To facilitate this practice, most manufacturers now provide weight- or size-based scan techniques for pediatric patients.

Automatic Exposure Control (AEC). Another way in which to tailor a technique appropriately to patient size is to use CT AEC, now available on many scanners (and often referred to as auto-mA). In a fashion analogous to radiographic AEC, CT AEC automatically selects scan mA on the basis of patient attenuation estimated from scout views. This process automatically provides an appropriate technique not only for each patient but also for each individual slice (or each individual rotation during helical scans); for example, higher mA will be used through the diaphragm and abdomen than through slices containing more lung tissues. In clinical practice, the mA automatic selection process is usually based on a user-specified acceptable image noise level.

Rotational AEC. Some systems now allow mA adjustment not only for each slice or rotation but also for individual views (angles) during a single rotation. This feature is most useful for anatomic regions that are far from "round," such as the hips or shoulders. In these cases, image noise (and image quality) is dominated by the very low x-ray intensities transmitted though the lateral views of the patient. Conversely, patient dose tends to be dominated by the higher intensities penetrating through the patient from the anterior and posterior views. By increasing mA for the "thick" patient views to reduce noise and reducing mA for the "thin" patient views to reduce radiation dose, one may achieve equivalent image quality (relative to nonrotational AEC) with as much as a 50% dose reduction (*15*).

MSCT Beam Width and Radiation Dose. Because radiation doses are higher for thinner beam widths in MSCT (Table 1), thinner beam widths should be avoided when possible. For example, for a 4-slice scanner, the use of a detector collimation of 4 × 1 mm or 4 × 1.25 mm (total beam width of 4–5 mm) should be avoided unless off-axis reconstructions are planned (for which the thinner slices are superior). Similarly, for a 16-slice scanner, a detector collimation of 16 × 1 mm, 16 × 1.25 mm, or 16 × 1.5 mm will yield lower doses than a detector collimation of 16 × 0.5 mm, 16 × 0.625 mm, or 16 × 0.75 mm for both axial and helical MSCT scans (*16*).

ADVANTAGES, DATA ISSUES, AND THE FUTURE

Advantages of MSCT

The rapid adoption of MSCT technology testifies to its advantages over SSCT. The principal basis of its advantages can be stated as follows: MSCT allows large anatomic ranges to be scanned while simultaneously producing both thin and thick slices. The availability of thick (>4–5 mm) slices is important because they are generally preferred for primary interpretation as a result of their lower image noise. Acquiring thin slices is important for 2 reasons: they reduce or eliminate partial-volume streaks, and they allow for the production of high-quality off-axis (sagittal, coronal, or oblique) or 3-dimensional reconstructions, often with a spatial resolution equivalent to that within the plane of the slice (referred to as isotropic resolution).

Although SSCT could, in principle, acquire thin slices, total scan times and subsequent x-ray tube heating prevented practical thin-slice scanning with thicknesses of less than 2.5–3 mm, except for very limited anatomic ranges. Typical off-axis (coronal) reconstructions available for SSCT and for MSCT are compared in Figure 10. The quality of MSCT off-axis reconstructions is such that in some cases, CT image interpretation is beginning to migrate toward primary interpretation from off-axis rather than axial images.

Data Issues

The growth of MSCT has been accompanied by rapid growth in the numbers of images per examination. The large numbers of images associated with MSCT examinations render film-based interpretation impractical and essentially mandate the use of PACS for efficient and timely examination interpretation. Although it is certainly true that MSCT examination sizes (in terms of image counts) are much larger than those for SSCT, significant misunderstandings exist regarding the continued expansion of data as MSCT continues to evolve.

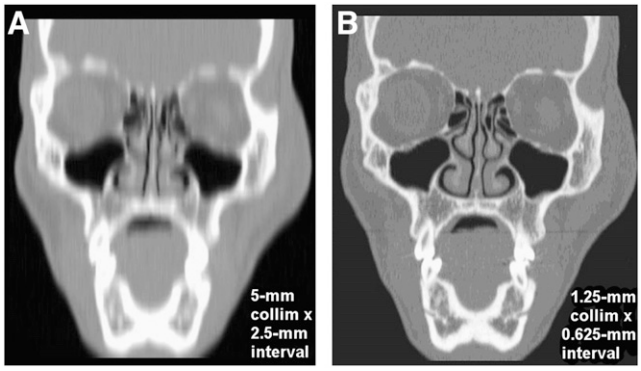

FIGURE 10. Coronal images formed from off-axis reformatting. (A) Thicker slices collected by SSCT lead to poor-quality, less efficacious off-axis images. (B) Thinner slices collected by MSCT lead to high-quality reformatted images, often with resolution equivalent to that within slice plane. collim = collimation.

With the introduction of 4-slice MSCT, the sizes of many (but not all) studies increased by 4- or 5-fold or more. This increase was attributable not so much to collecting 4 slices at once but rather to MSCT scanning of large sections of anatomy with thin slices (2.5 mm or less), relative to SSCT scanning of the same anatomy with 5- to 10-mm slices. For example, covering a 40-cm scan range with contiguous 5-mm slices (whether acquired axially or helically) would generate 80 images. MSCT scanning of the same range with a collimation of 4 × 1.25 mm to produce both 1.25- and 5-mm slices would generate 400 images: 320 images with a thickness of 1.25 mm and 80 images with a thickness of 5 mm.

The reason for the large increase in image counts in the example just given is coverage of the same anatomic range with both thin and thick slices rather than simultaneous acquisition of multiple images. A 16-slice scanner covering the same anatomy with a collimation of 16 × 1.25 mm (again reconstructed into both 1.25- and 5 mm slices) would also yield 400 images—but it would obtain them 4 times faster (assuming an equivalent rotation time). On the other hand, if the same 40-cm area were scanned with a collimation of 16 × 0.625 mm to produce 0.625- and 5 mm slices, then 720 images would result (640 images of 0.625-mm slices and 80 images of 5-mm slices). A 64-slice machine scanning the same area to produce 0.625- and 5-mm slices would also generate 720 images. In general, the numbers of images produced by MSCT are associated with detector collimation and how the data are used rather than with the numbers of simultaneously acquired slices. How many slices an MSCT scanner can acquire simultaneously affects how fast images are acquired—not how many images are acquired.

Although scanners capable of collecting more than 64 slices are now either available or in clinical trials, it is unlikely that detector element size and therefore minimum detector collimation will continue to shrink. Because current element sizes (typically 0.5–0.75 mm) are already comparable to detector element sizes within the slice plane (see, for example, the in-plane and *z*-direction dimensions of the 0.625-mm elements in Fig. 5), still-smaller *z*-axis elements lead to diminishing returns. Thus, except perhaps for new and special applications, such as cardiac CT angiography (CTA) (see next section), the numbers of images in MSCT examinations are unlikely to increase significantly.

Cardiac MSCT

The application that currently seems to be driving state-of-the-art MSCT is CTA. Except for cardiac screening applications with electron-beam CT, cardiac imaging has been a difficult hurdle for CT because of its demanding performance requirements. In most cases, the optimal time for scan data collection is during a relatively motionless-heart window of time (lasting about 175 ms for a heart beating at 60 beats per minute) occurring at approximately 65%–75% of the R-R interval. Because of this very short time interval, CTA examinations are electrocardiographically gated helical scans with data acquired during the same heart phase over several heartbeats. Small beam pitches (0.25 or less) are used to ensure the collection of data for slice interpolation during appropriate rotational tube positions. For optimal examination quality, data associated with the reconstruction of individual slices should be collected during a single beat, with the entire heart being covered in as few beats as possible (*17*).

Steps toward meeting these requirements have led to faster rotation times and larger *z*-axis fields of view. Normally, individual cardiac axial images are reconstructed from "half-scan" data (i.e., data collected over a half rotation [180°] plus the fanbeam angle, or about 210°) rather than from 360° of data. Currently, the fastest rotation times are on the order of 1/3 s. At this speed, half-scan data can often be acquired during a single beat or, at most, 2 beats. Further speed improvements are difficult to achieve because of both mechanical stresses and x-ray output limitations. A possible solution now in clinical use by one manufacturer involves 2 x-ray tubes and detector arrays, so that each tube–detector pair need only complete a quarter rotation (taking about 85 ms) to acquire half-scan data.

To allow coverage of the entire heart in as few beats as possible, *z*-axis fields of view have increased to a current maximum of 40 mm. One manufacture has begun clinical trials of a 256-slice MSCT scanner with a 128-mm *z*-axis field of view (but with a slower [0.5-s] rotation time) (*18*).

CONCLUSION

MSCT will continue to evolve. Most likely, future MSCT technology advances will be aimed at improving CTA. Except for CTA and a few other examinations that benefit from greater speed or large *z*-axis fields of view, it is unclear at this point whether additional, significant clinical advantages will accrue beyond those of 16-slice MSCT.

Because *z*-axis resolution and scan quality are essentially identical, the gain seems to be mostly in scan times, which are already extraordinarily short for 16-slice scanners. Whether 16 slice, 64 slice, or beyond, MSCT will continue to grow in importance as a primary diagnostic imaging tool.

APPENDIX

z-Spacing of Parallel Opposed Rays in Helical CT

The spacing along the *z*-axis of measurements (samples) used to interpolate helical CT slices affects the presence of helical artifacts in images: the smaller the spacing, the less severe the artifacts. Although diagrams such as those in Figures 7 and 8 are often used to illustrate helical *z*-spacing, they are somewhat misleading. Parallel opposed rays used for interpolation (or *z* filtering) are separated by a half rotation (180°) only for detectors at the center of the fanbeam detector array (i.e., at the center of the array within the plane of the slice). Thus, parallel opposed rays occur when the x-ray tube is on the exact opposite side of the patient.

For all other detectors, parallel opposed rays occur at some other point during the rotation (either less than or more than a half rotation), depending on the location of the detector within the fanbeam array: the closer the detector is to the end of the array, the farther from a half rotation the parallel opposed ray occurs.

REFERENCES

1. Goldman L. Principles of CT and evolution of CT technology. In: Goldman LW, Fowlkes JB, eds. *Categorical Course in Diagnostic Radiology Physics: CT and US Cross-Sectional Imaging*. Oak Brook, IL: Radiological Society of North America; 2000:33–52.
2. McCollough C, Zink F. Performance evaluation of a multi-slice CT system. *Med Phys.* 1999;26:2223–2230.
3. Flohr TG, Schaller S, Stierstorfer K, Bruder H, Ohnesorge BM, Schoepf UJ. Multi-detector row CT systems and image-reconstruction techniques. *Radiology.* 2005;235:756–773.
4. Lewis M, Keat N, Edyvean S. 16 Slice CT scanner comparison report version 14. Report 06012, Feb-06. Available at: http://www.impactscan.org/reports/Report06012.htm. Accessed March 26, 2008.
5. Lewis M, Keat N, Edyvean S. 32 - 64 Slice CT scanner comparison report version 14. Report 06013, Feb-06. Available at: http://www.impactscan.org/reports/Report06013.htm. Accessed March 26, 2008.
6. Goldman LW. Principles of CT: radiation dose and image quality. *J Nucl Med Technol.* 2007;35:213–225.
7. Hsieh J. Investigation of the slice sensitivity profile for step-and-shoot mode multi-slice computed tomography. *Med Phys.* 2001;28:491–500.
8. Goldman LW. Principles of CT and CT technology. *J Nucl Med Technol.* 2007;35:115–128.
9. Kalender W. Principles and performance of single- and multislice spiral CT. In: Goldman LW, Fowlkes JB, eds. *Categorical Course in Diagnostic Radiology Physics: CT and US Cross-Sectional Imaging*. Oak Brook, IL: Radiological Society of North America; 2000:127–142.
10. Hu H. Multi-slice helical CT: scan and reconstruction. *Med Phys.* 1999;26:5–18.
11. Wang G, Vannier M. The effect of pitch in multislice spiral/helical CT. *Med Phys.* 1999;26:2648–2653.
12. La Riviere P, Pan X. Pitch dependence of longitudinal sampling and aliasing effects in multi-slice helical computed tomography (CT). *Phys Med Biol.* 2002; 47:2797–2810.
13. Nickoloff E, Dutta A, Lu Z. Influence of phantom diameter, kVp and scan mode upon computed tomography dose index. *Med Phys.* 2003;30:395–402.
14. Siegel M, Schmidt B, Bradly D, Suess C, Hildebolt C. Radiation dose and image quality in pediatric CT: effect of technical factors and phantom size and shape. *Radiology.* 2004;233:515–522.
15. Kalender W, Heiko W, Suess C. Dose reduction in CT by anatomically adapted tube current modulation. II. Phantom measurements. *Med Phys.* 1999;26:2248–2253.
16. Mahesh M, Scatarige J, Copper J, Fishman E. Dose and pitch relationship for a particular multislice CT scanner. *AJR.* 2001;177:1273–1275.
17. Hoffmann U, Ferencik M. Cury RC, Pena AJ. Coronary CT angiography. *J Nucl Med.* 2006;47:797–806.
18. Shinichiro M, Endo M, Tsunoo T, et al. Physical performance evaluation of a 256-slice CT-scanner for four-dimensional imaging. *Med Phys.* 2004;31: 1348–1356.